



A variable temperature EPR study of the manganites $(\text{La}_{1/3}\text{Sm}_{2/3})_{2/3}\text{Sr}_x\text{Ba}_{0.33-x}\text{MnO}_3$ ($x=0.0, 0.1, 0.2, 0.33$): Small polaron hopping conductivity and Griffiths phase

Sushil K. Misra^{a,*}, Sergey I. Andronenko^{a,1}, Saket Asthana^b, Dharendra Bahadur^c

^a Physics Department, Concordia University, 1455 de Maisonneuve Boulevard West, Montreal, Quebec, Canada H3G 1M8

^b Physics Department, Indian Institute of Technology, Hyderabad 502205, Andhra Pradesh, India

^c Department of Metallurgy, Indian Institute of Technology, Powai, Mumbai 400076, India

ARTICLE INFO

Article history:

Received 2 December 2009

Received in revised form

19 April 2010

Available online 7 May 2010

Keywords:

Doped manganites

Electron paramagnetic resonance (EPR)

Small-polaron hopping

Griffiths phase

ABSTRACT

Four manganite samples of the series, $(\text{La}_{1/3}\text{Sm}_{2/3})_{2/3}\text{Sr}_x\text{Ba}_{0.33-x}\text{MnO}_3$, with $x=0.0, 0.1, 0.2$ and 0.33 , were investigated by X-band (~ 9.5 GHz) electron paramagnetic resonance (EPR) in the temperature range 4–300 K. The temperature dependences of EPR lines and linewidths of the samples with $x=0.0, 0.1$ and 0.2 , containing Ba^{2+} ions, exhibit similar behavior, all characterized by the transition temperatures (T_C) to ferromagnetic states in the 110–150 K range. However, the sample with $x=0.33$ (containing no Ba^{2+} ions) is characterized by a much higher $T_C=205$ K. This is due to significant structural changes effected by the substitution of Ba^{2+} ions by Sr^{2+} ions. There is an evidence of exchange narrowing of EPR lines near T_{min} , where the linewidth exhibits the minimum. Further, a correlation between the temperature dependence of the EPR linewidth and conductivity is observed in all samples, ascribed to the influence of small-polaron hopping conductivity in the paramagnetic state. The peak-to-peak EPR linewidth was fitted to $\Delta B_{\text{pp}}(T) = \Delta B_{\text{pp,min}} + A/\text{Texp}(-E_a/k_B T)$, with $E_a=0.09$ eV for $x=0.0, 0.1$ and 0.2 and $E_a=0.25$ eV for $x=0.33$. From the published resistivity data, fitted here to $\sigma(T) \propto 1/T \exp(-E_\sigma/k_B T)$, the value of E_σ , the activation energy, was found to be $E_\sigma=0.18$ eV for samples with $x=0.0, 0.1$ and 0.2 and $E_\sigma=0.25$ eV for the sample with $x=0.33$. The differences in the values of E_a and E_σ in the samples with $x=0.0, 0.1$ and 0.2 and $x=0.33$ has been ascribed to the differences in the flip-flop and spin-hopping rates. The presence of Griffiths phase for the samples with $x=0.1$ and 0.2 is indicated; it is characterized by coexistence of ferromagnetic nanostructures (ferrons) and paramagnetic phase, attributed to electronic phase separation.

© 2010 Elsevier B.V. All rights reserved.

1. Introduction

The compounds $(\text{La}_{1/3}\text{Sm}_{2/3})_{2/3}\text{Sr}_x\text{Ba}_{0.33-x}\text{MnO}_3$ have the common formula $\text{A}_{1-y}\text{B}_y\text{MnO}_3$ (where $\text{A}=\text{La, Sm, Pr}$, or another rare-earth ion, and $\text{B}=\text{Ca, Ba, Sr}$; $y=1/3$). They are members of a large series of rare-earth manganites exhibiting giant magnetoresistance. Their transport, magnetic and structural properties are very sensitive to the substitution of trivalent rare-earth ion (A^{3+}), as well as that of divalent ions (B^{2+}). These compounds have been the subject of several investigations, including FMR/EPR investigations of Mn ions. (See Refs. [1–25] in the reference section, where the details of particular investigations have been included. Here FMR stands for ferromagnetic resonance.) Special attention

was given to the spin dynamics of the Mn ions near the magnetic phase transition, and explanation of the pseudolinear increase in EPR linewidth in the paramagnetic state of these compounds above the Curie temperature. Despite all these efforts, the magnetic behavior of these compounds has not been fully understood as yet.

The effect of substitution of the Sr^{2+} ion, with the ionic radius of 1.12 \AA , for the Ba^{2+} ion, with the larger ionic radius of 1.34 \AA , has been investigated here on the EPR spectra in the manganites $(\text{La}_{1/3}\text{Sm}_{2/3})_{2/3}\text{Sr}_x\text{Ba}_{0.33-x}\text{MnO}_3$, $x=0.0, 0.1, 0.2$, and 0.33 . This substitution affects the structure of these compounds leading to a deviation from the ideal cubic structure, the degree of which is dependent on the ionic radius of the substituting divalent cation. The amount of substitution governs the fractional contents of the Mn^{3+} and Mn^{4+} ions present in these samples. The change in the average size of the cation at the B site of these perovskites results in large changes in their transport and magnetic properties due to modification of the Mn–O–Mn bond angles and Mn–O distances, thereby influencing the e_g electron hopping between the Mn^{3+}

* Corresponding author.

E-mail address: skmisra@alcor.concordia.ca (S.K. Misra).

¹ Present address: Physics Department, Kazan State University, Kazan, 42008, Russia.

and Mn^{4+} states. Also, such distortion of the bond angles and distances gives rise to competing superexchange and double-exchange interactions, causing electronic phase separation. It is noted here that increasing Ba content leads to increasing disorder in the system, and therefore to a possible appearance of enhanced spin-glass like phase in these samples. Further, in these compounds, diamagnetic La ions are partly substituted by the paramagnetic Kramers Sm^{3+} ions, which strongly affects the magnetic states of these compounds below their phase transitions: where there occurs a competition between the ferro and antiferromagnetic states, which, in turn, affects their magnetoresistance [1–10]. Asthana et al. [9] reported detailed investigations of the magnetic susceptibility and conductivity in the temperature range 4–320 K in these compounds, whereas Huanyin et al. [1] investigated the influence of heavy doping of Sm in $\text{La}_{0.67}\text{Sr}_{0.33}\text{MnO}_3$.

This paper reports a detailed X-band (~ 9.5 GHz) electron paramagnetic resonance (EPR) study of the manganite compounds $(\text{La}_{1/3}\text{Sm}_{2/3})_{2/3}\text{Sr}_x\text{Ba}_{0.33-x}\text{MnO}_3$ ($x=0.0, 0.1, 0.2$ and 0.33) in the temperature range 4–300 K. Apart from studying the occurrence of Griffiths phase in the samples with $x=0.1$ and 0.2 , an important aim of the present work is to understand the behavior of the broadening of EPR lines in the paramagnetic state and to investigate the ferromagnetic nanostructures (ferrons) in these compounds.

2. Experimental arrangement

A Bruker ER-200D SRC EPR X-band spectrometer, equipped with an Oxford helium-flow cryostat for temperature variation in the liquid-helium temperature range for 4–150 K, as well as a Bruker temperature controller for variation in the liquid-nitrogen temperature range 120–300 K, was used to investigate the manganite samples $(\text{La}_{1/3}\text{Sm}_{2/3})_{2/3}\text{Sr}_x\text{Ba}_{0.33-x}\text{MnO}_3$. It is noted here that with the Oxford cryostat, one goes to the lowest temperature (4 K) first, and then all measurements are carried out with increasing temperature, whereas with the Bruker cryostat the measurements are made for temperatures decreasing from room temperature. The difference in the direction of temperature change does lead to some hysteresis in the EPR linewidth and line positions. This is similar to that observed in YBaMn_2O_6 , where the structural phase-transition temperature T_t determined during cooling was found to be less than the phase transition temperature determined during heating. [4]

3. EPR spectra

3.1. Phase transitions from paramagnetic to magnetically ordered phase

The variation of the first-derivative EPR spectra with temperature for these samples is shown in Figs. 1, 2, 3 and 4 for the samples with $x=0.0, 0.1, 0.2$ and 0.33 , respectively. They exhibit essentially the same behavior of the main, intense line as the temperature is lowered. The phase-transition temperatures from the magnetically ordered states to the paramagnetic state, at which spontaneous magnetization drops to zero, as determined from magnetization data [9], are 96, 112, 127 and 203 K, for $x=0.0, 0.1, 0.2$ and 0.33 , respectively. For all these samples, $g \sim 2.0$ for the EPR line in the paramagnetic phase. For the sample with $x=0.33$, two lines,—the narrow one situated in the 2200–2800 G range and the broader one centered around 3500 G, were observed clearly below 210 K, as seen in Fig. 4. The broader line disappears below 190 K, at which the sample becomes fully

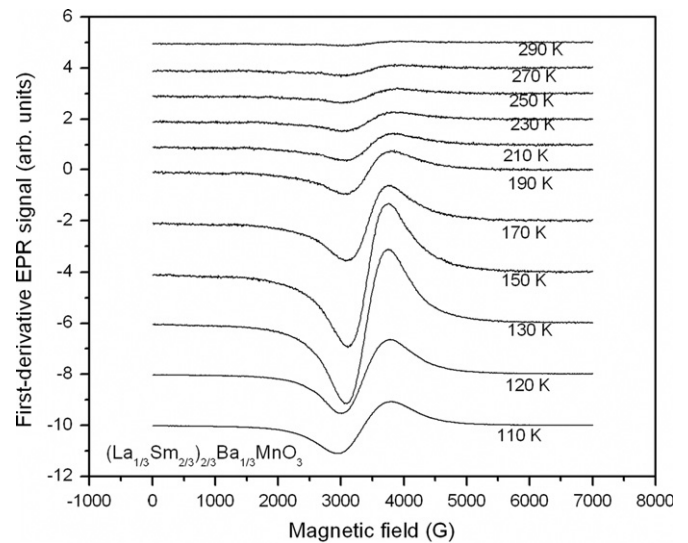


Fig. 1. Variation of EPR spectra of $(\text{La}_{1/3}\text{Sm}_{2/3})_{2/3}\text{Ba}_{1/3}\text{MnO}_3$ sample ($x=0.0$) versus temperature from 4 to 290 K. EPR lines below and above 110 K were recorded using the Oxford and Bruker temperature controllers, respectively.

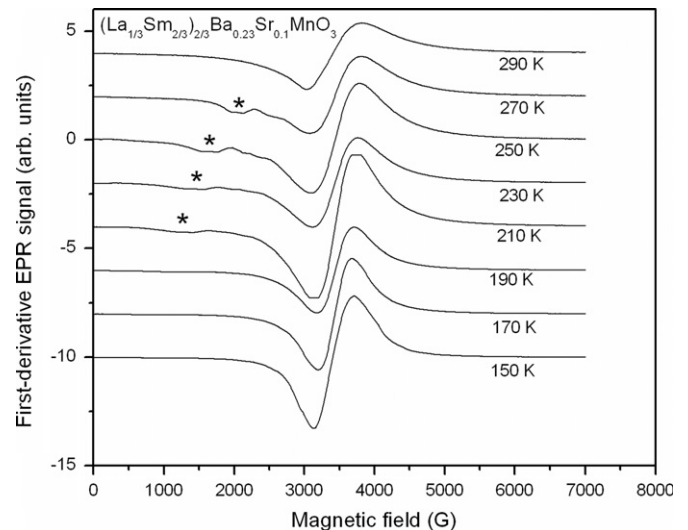


Fig. 2. Variation of EPR spectra of $(\text{La}_{1/3}\text{Sm}_{2/3})_{2/3}\text{Ba}_{0.23}\text{Sr}_{0.1}\text{MnO}_3$ sample ($x=0.1$) versus temperature from 4 to 290 K. The second signal in the region 230–270 K is clearly seen, and indicated by a star. EPR lines below and above 150 K were recorded using the Oxford and Bruker temperature controllers, respectively.

ferromagnetic. The narrower EPR line starts to move to lower magnetic fields with decreasing temperature below 205 K in the ferromagnetic region. In Fig. 5, the overlap of broad and narrow EPR lines is successfully simulated as a weighed sum of two EPR lines, one of these is situated at $g=2.04$ (paramagnetic), whereas the second one (ferromagnetic phase) is situated at a higher g value, varying from 2.5 at 210 K to 2.9 at 200 K as the temperature decreases. The second line has the Lorentzian shape. As revealed by this simulation, the relative contribution of the first line decreases in this temperature region, accompanied by the contribution of the second line increasing sharply, from 13% at 210 K to 60% at 200 K. The presence of two lines at the same temperature, one paramagnetic and the other ferromagnetic, representing two different magnetic phases, is a clear evidence of phase separation in this compound near the magnetic phase transition. This is due to the varying distribution of Sr^{2+} ions over the sample, which, in turn, leads to fluctuations of $\text{Mn}^{3+}/\text{Mn}^{4+}$

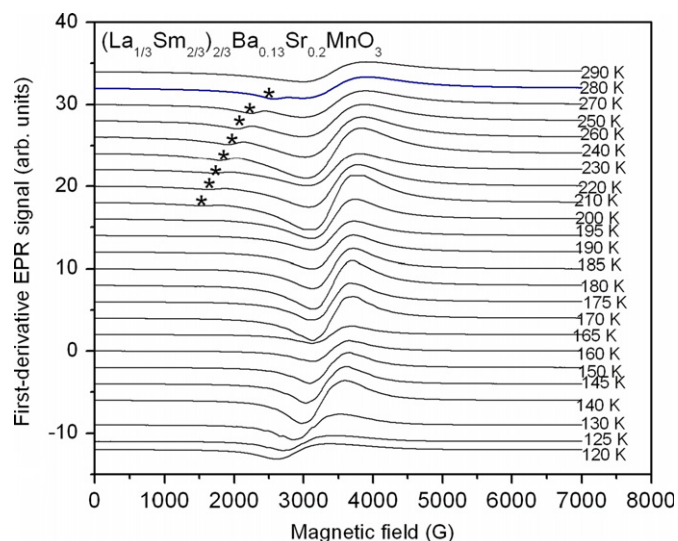


Fig. 3. Variation of EPR spectra of $(\text{La}_{1/3}\text{Sm}_{2/3})_{2/3}\text{Ba}_{0.13}\text{Sr}_{0.20}\text{MnO}_3$ sample ($x=0.2$) versus temperature from 120 to 290 K. The second signal in region 210–280 K is clearly seen, and indicated by a star. EPR lines above 110 K were recorded using the Bruker temperature controller.

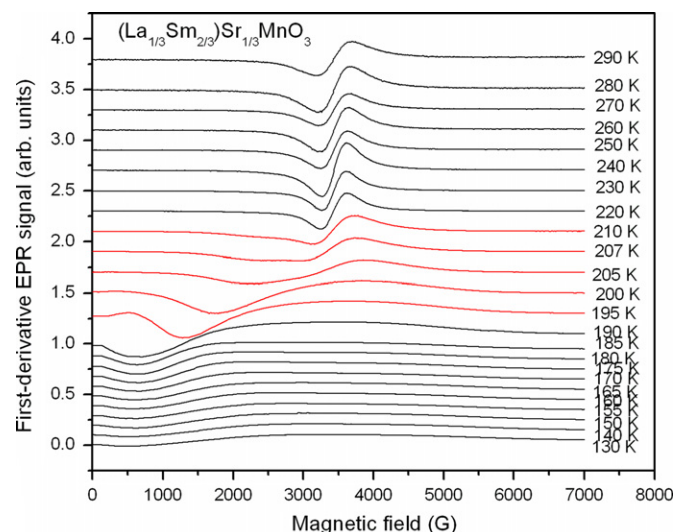


Fig. 4. EPR spectra of $(\text{La}_{1/3}\text{Sm}_{2/3})_{2/3}\text{Sr}_{1/3}\text{MnO}_3$ sample ($x=0.33$) versus temperature near the phase transition region 130–290 K.

distribution over the sample, and thus to the coexistence of paramagnetic and ferromagnetic phases in the close vicinity of the phase transition.

Griffiths phase. For the samples with $x=0.1$ and 0.2 , an additional weak EPR line over and above the more intense line was observed due to the Griffiths phase as seen in Figs. 2 and 3. The position of the weak line moves towards lower fields from about 2500 G to a bit below 2000 G with decreasing temperature from 270 to 200 K. The linewidths of these weak lines for the two samples are 250–300 G, not changing much over the temperature range of their occurrence. They are due to the existence of ferromagnetic nanostructures (ferrons) due to the Griffiths phase [26], wherein the formation of nuclei of the ferromagnetic phase depends on the disorder parameter. The occurrence of the Griffiths phase in these compounds is further justified as follows. The magnetic susceptibility for the samples with $x=0.1$ and 0.2 does not follow the Curie–Weiss law. The nuclei of the ferromagnetic phase at the nanosized level are formed

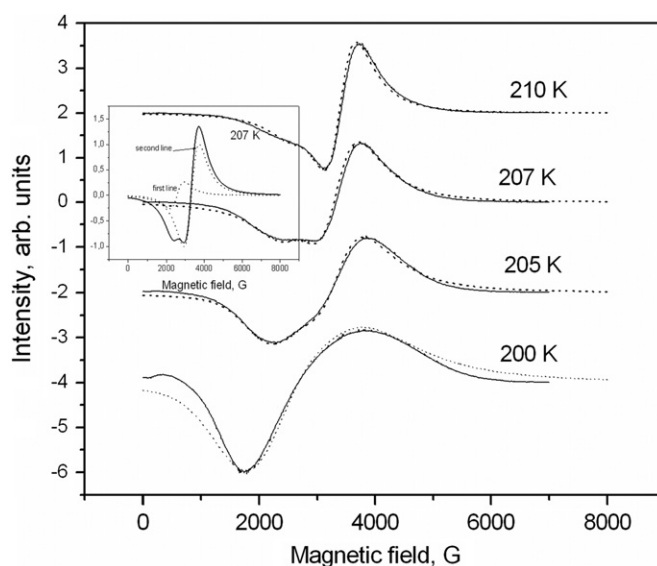


Fig. 5. EPR spectra of $(\text{La}_{1/3}\text{Sm}_{2/3})_{2/3}\text{Sr}_{1/3}\text{MnO}_3$ sample ($x=0.33$) versus temperature near the phase transition region 205–210 K. The solid lines are experiment, whereas the simulations are shown by dotted lines. In the inset, the solid line is the sum of two dotted simulated lines.

within the paramagnetic phases below the so-called Griffiths temperature (T_G) and above the Curie temperature (T_C) of the compounds. The Sr^{2+} and Ba^{2+} ions cause disorder here. Their replacement of the La^{3+} ions leads to creation of holes located at the positions of the Mn, or oxygen, ions. They migrate to the sites of the Mn^{3+} ions, causing polarization of the direction of spins, leading to the formation of ferromagnetically ordered nanostructures. These ferron nanostructures may cause phase separations in the manganites [21]. In the samples with $x=0.1$ and 0.2 , the Griffiths temperature (T_G) was estimated to be about 290 K from the EPR data, being the temperature below which the ferromagnetic lines appear. Similar weak ferromagnetic EPR signals were reported in $\text{La}_{1-x}\text{Ba}_x\text{MnO}_3$ for $0.05 < x < 0.3$ below 340 K by Eremina et al. [21] for which $T_C=340$ K, which is much higher than $T_C=270$ K for $\text{La}_{1-x}\text{Sr}_x\text{MnO}_3$ [22]. These are the inhomogeneities, arising from the variable Mn oxidation state, which lead to the electronic phase separation at the nano-scale length [6,7].

3.2. EPR linewidths

The temperature variations of the peak-to-peak linewidths, ΔB_{pp} , of the first-derivative EPR signal as functions of T for the four samples are shown in Fig. 6. For the samples with $x=0.0, 0.1$ and 0.2 , the EPR linewidth decreased gradually as the temperature was reduced from 300 K in the paramagnetic phase, but increased sharply below 120 K. In all the samples, the linewidths are affected by exchange narrowing and hopping, as described below.

3.2.1. T_{min} and $\Delta B_{pp,min}$

For all four samples, ΔB_{pp} decreases almost linearly with decreasing T above T_{min} , at which the minimum $\Delta B_{pp,min}$ of the linewidth occurs. Upon decreasing T below T_{min} ΔB_{pp} increases sharply, accompanied by a distortion in the lineshape. Above T_{min} , the spectrum exhibits a structureless single line, implying that for $T > T_{min}$ the sample is paramagnetic. The temperature dependence and linewidth of the sample without Ba ions ($x=0.33$) are at variance from those exhibited by the other three samples ($x=0.0, 0.1$ and 0.2), containing Ba^{2+} ions. For this sample, $T_{min}=240$ K, which is considerably higher than those for the other

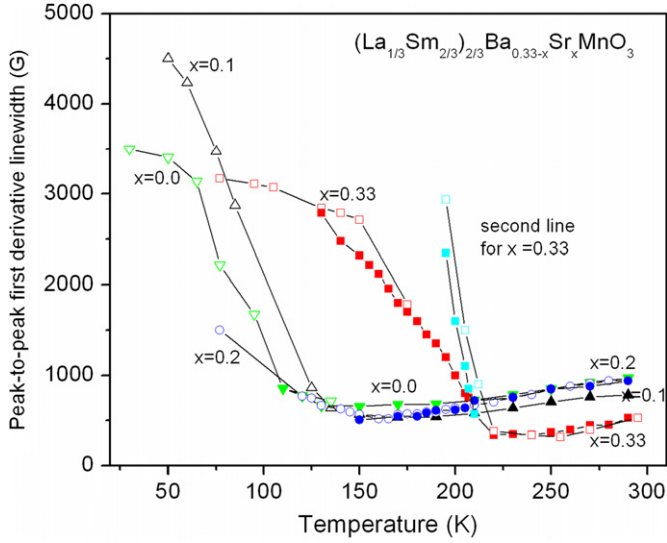


Fig. 6. Peak-to-peak EPR linewidth of the manganite samples versus temperature. Here the EPR linewidths for the samples with $x=0.0, 0.1, 0.2$ and 0.33 are indicated by down triangles, up triangles, circles and squares, respectively. The open and closed symbols indicate data obtained for increasing and decreasing temperature changes, produced by Bruker and Oxford controllers, respectively. The second signal in the range 190–210 K for $x=0.33$ sample indicated by cyan squares.

samples (150, 170 and 170 K for $x=0.0, 0.1$ and 0.2 , respectively). This is explained as follows. T_c , the Curie temperature as determined from the temperature dependence of the magnetization for each sample under investigation in Section. 2 [9], increases with increase in the Sr content due to increase in the overlap integral of electron densities of Mn and O ions, leading to an increase in ferromagnetic ordering. Increasing Ba content diminishes the long-range ferromagnetic ordering and enhances frustration due to competition between ferromagnetic and antiferromagnetic ordering, which causes phase separation in these systems. The local atomic disorder increases with decreasing Sr content, as a result of which the ferromagnetic interactions become weaker as compared to those with antiferromagnetic interactions [9].

3.2.2. Linewidth mechanisms

The peak-to-peak first-derivative linewidth for $T > T_{\min}$, for the various samples can be expressed as a sum of two terms, one of which is temperature-independent, whereas the other is temperature-dependent, so that $\Delta B_{pp} = \Delta B_{pp,\min} + \Delta B_{pp}(T)$.

Temperature-dependent EPR linewidth $\Delta B_{pp}(T)$: It is proportional to the magnetic susceptibility, and is given as [2–5]

$$\Delta B_{pp}(T) = [\chi_0(T)/\chi(T)]\Delta B_{pp}(\infty) \quad (1)$$

where $\chi_0(T) \propto T^{-1}$ is the free spin (Curie) susceptibility; χ is the measured susceptibility; and $\Delta B_{pp}(\infty)$ is the temperature-independent value. Huber et al. [3] calculated the influence of exchange narrowing, using a general expression for the relaxation rate of the total spin. This approach is based on the memory-function formalism developed by Mori [27], calculating $\Delta B_{pp}(T)$ as a function of the second- and fourth-order moments, M_2 and M_4 , and concluding that the main reason for broadening is the variation of the orthorhombic crystal-field parameters over the various Mn ions. The influence of the antisymmetric exchange interaction (Dzialozhinsky–Moriya) on EPR linewidth was found to be important [3]. However, the calculations showed very little influence of the dipole–dipole interactions in these manganite compounds, in agreement with the calculations of Huber et al. [2,3].

Hopping conductivity: It is attributed to the temperature-dependent spin-lattice interactions [11–14], including those due to single-phonon spin-lattice relaxation [28] and bottle-necked spin relaxation between the Mn^{3+} and Mn^{4+} ions present in the samples [12]. Causa et al. [15] studied the effect of Mn^{3+} and Mn^{4+} ions on the EPR signal, observing a deviation of the double-integrated first-derivative EPR intensity (area under the absorption line) from the Curie–Weiss behavior in the paramagnetic region. The explicit form of $\Delta B_{pp}(T)$, based on the model of EPR linewidth broadening due to the hopping process, is discussed as follows. A linear relation between the EPR linewidth (ΔB_{pp}) and conductivity is often observed in systems exhibiting hopping conductivity [27]. The hopping rate of the charge carriers limits the lifetime of the spin state. One of the contributions to the conductivity in manganites has been ascribed to hopping by Chen et al. [23]. The consequent EPR line broadening and increase in conductivity are proportional to the hopping rate [29]. The temperature dependence of ΔB_{pp} above T_{\min} is very similar to that of the electrical conductivity observed in manganite [24]. Accordingly, the following expression [2,3] was used here to fit the EPR linewidth for $T > T_{\min}$:

$$\Delta B_{pp}(T) = \Delta B_{pp,\min} + \frac{A}{T} \exp(-E_a/k_B T) \quad (2)$$

The best-fit parameters are: $\Delta B_{pp,\min} = 334, 505, 540, 648$ G, and $E_a = 0.26, 0.089, 0.090$ and 0.089 eV for the samples with $x = 0.33, 0.2, 0.1$ and 0.0 , respectively. For comparison, the temperature dependence of the measured electrical resistivity, as reported by Asthana et al. [9], is shown in Fig. 7, according to which both the EPR linewidth and conductivity exhibit similar temperature dependences. In the paramagnetic regime, the conductivity (σ) values for the manganite samples are dominated by adiabatic hopping motion of small polarons [25,30], whose temperature dependence is given by

$$\sigma(T) \propto (1/T) \exp(-E_\sigma/k_B T) \quad (3)$$

where E_σ is the activation energy. The resistivity data plotted in Fig. 7 for $T > 200$ K were fitted to this expression, obtaining the values $E_\sigma = 0.25, 0.18, 0.18$ and 0.18 eV for the samples with $x = 0.33, 0.2, 0.1$ and 0.0 , respectively. A comparison of E_a and E_σ

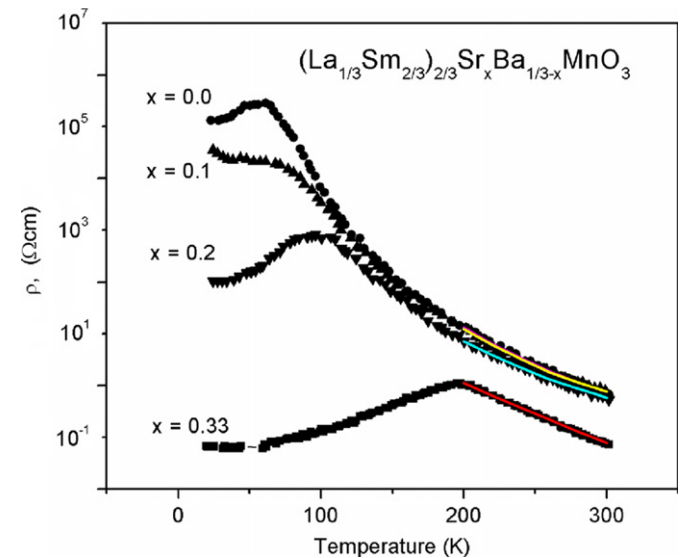


Fig. 7. Variation of resistivity with temperature for $(La_{1/3}Sm_{2/3})_{2/3}Sr_xBa_{1/3-x}MnO_3$ samples. The data points for the sample with $x=0.0$ are represented by closed circles, those for the sample with $x=0.1$ by up triangles, those for the sample with $x=0.2$ by down triangles and those for the sample with $x=0.33$ by closed squares. The continuous lines represent fitting of the data points to Eq. (3).

values determined here reveals that these two values are equal for the sample with $x=0.33$ without Ba^{2+} ions, whereas the value of E_σ is about twice that of E_a for the samples with $x=0.0, 0.1$ and 0.2 , in which there is a partial replacement of Sr^{2+} ions by Ba^{2+} ions. They ascribed the differences in the E_a and E_σ values to the mechanisms responsible for these processes, which are the slower spin-lattice dynamics near the Curie point that determines E_a values and the hopping motion that determines E_σ values. Specifically, the temperature dependences of the resistivity and EPR linewidth in the paramagnetic region are due to small-polaron hopping, wherein polarons formed near the Curie point are located between the Mn^{3+} and Mn^{4+} ions. They are mediated by the double-activated hopping of the itinerant e_g electrons through the O^{2-} ions. The present results on the manganite samples are in accordance with those reported by Ulyanov et al. [20] for the manganite $Pr_{0.7}Ba_{0.3}MnO_3$, where similar activation energies were obtained, estimating E_σ from the resistivity data to be 0.16 eV and E_a values from the EPR linewidth and intensity data to be 0.09 and 0.11 eV, respectively.

The structure of $(La_{1/3}Sm_{2/3})_{2/3}Sr_xBa_{0.33-x}MnO_3$ was investigated by Asthana et al. [9]. They found orthorhombic structure at room temperature (paramagnetic region) for all samples. The structure changes towards pseudocubic with decreasing Sr content. Considerable decrease in a, b, c parameters was observed for samples with x between 0.2 and 0.33. The peculiarities of structures of $(La_{1/3}Sm_{2/3})_{2/3}Sr_xBa_{0.33-x}MnO_3$ with and without Ba may explain the difference in the E_a and E_σ values for $x < 0.33$. The difference in the E_a and E_σ values in the samples $(La_{1/3}Sm_{2/3})_{2/3}Sr_xBa_{0.33-x}MnO_3$ with $x=0.33$ and $x=0.0, 0.1$ and 0.2 is explained as follows. According to Huber et al. [2], in manganites one can consider the existence of two separate systems of electrons: (i) core spins ($S=3/2$), which are responsible for magnetism, and (ii) e_g polarons, which are responsible for conductivity. Both systems of electrons are thermally activated. This leads to temperature dependence of the conductivity, as well as that of the EPR intensity and linewidth. They proposed that hopping weakens Hund's rule correlations between the core spins and the spins of the e_g electrons that lead to parallel alignment in $LaMnO_3$. This correlation diminishes with increasing $Mn^{4+}-O-Mn^{3+}$ distance, leading to the large difference in energy of thermal activation for the samples with $x < 0.33$. For the sample with $x=0.33$ with more compact structure, the correlation between these two electron systems is stronger, and almost equal values of E_a and E_σ are observed for this sample. If these two systems of spins are separate systems, activation energies for each of them are different. This results in a smaller value of E_a , as compared to E_σ for the samples containing Ba ions. It is suggested here that the symmetry of the Mn magnetic sublattice for $x=0.33$ is different from that for $x=0.0, 0.1$, and 0.2 and that there occurs some kind of structural phase transition with increasing Ba content. To verify this, more detailed investigations of the magnetic and structural properties of $(La_{1/3}Sm_{2/3})_{2/3}Sr_xBa_{0.33-x}MnO_3$ compounds in the range $0.2 < x < 0.33$ are required.

4. Concluding remarks

The salient features of the EPR study on the manganite samples of $(La_{1/3}Sm_{2/3})_{2/3}Sr_xBa_{0.33-x}MnO_3$ presented in this paper are as follows:

- (i) The EPR linewidth is influenced by the processes of temperature-independent exchange narrowing and temperature-dependent hopping conductivity.
- (ii) The presence of Griffiths phase, characterized by the coexistence of ferron nanostructures and paramagnetic bulk state,

was clearly observed in the samples with $x=0.1$ and 0.2 below 300 K.

- (iii) Spin-lattice dynamics slows down in the samples containing Ba^{2+} ions, that is those with $x=0.0, 0.1$ and 0.2 , leading to the differences in the values of the activation energies E_a and E_σ .

It is hoped that the results presented in this paper would stimulate further quantitative studies of these manganites involving conductivity and magnetic susceptibility measurements.

Acknowledgments

S. K. M. is grateful to the Natural Sciences and Engineering Research Council (NSERC) of Canada for partial financial support.

References

- [1] Guo Huanyin, Liu Ning, Yan Guoqing, Tong Wei, Transport property of $La_{0.67-x}Sm_xSr_{0.33}MnO_3$, at heavy samarium doping ($0.40 \leq x \leq 0.60$), J. Rare Earths 24 (2) (2006) 206–213.
- [2] D.L. Huber, D. Laura-Ccahuana, M. Tovar, M.T. Causa, Electron spin resonance linewidth, susceptibility, and conductivity in doped manganites, J. Magn. Mater. 310 (2) (2007) e604–e606 part 1.
- [3] D.L. Huber, G. Alejandro, A. Caneiro, M.T. Causa, F. Prado, M. Tovar, S.B. Oseroff, EPR linewidths in $La_{1-x}Ca_xMnO_3$: $0 < x < 1$, Phys. Rev. B 60 (17) (1999) 12155–12161.
- [4] D. Zakharov, J. Deisenhofer, H.-A. Krug von Nidda, A. Loidl, T. Nakajima, Y. Ueda, Electron spin resonance across the charge-ordering transition in $YBaMn_2O_6$, Phys. Rev. B 78 (2008) 235105.
- [5] B.I. Kochelaev, E. Shilova, J. Deisenhofer, H.-A. Krug von Nidda, A. Loidl, A.A. Mukhin, A.M. Balbasov, Phase transitions and spin-relaxation in $La_{0.95}Sr_{0.05}MnO_3$, Modern Phys. Lett. B 17 (10/12) (2003) 459–467.
- [6] D. Bahadur, M. Yewondwossen, Z. Koziol, M. Foldeaki, R.A. Dunlap, Physical properties of the giant magnetoresistive perovskite system $La-Er-Ca-Mn-O$, J. Phys. Condens. Matter. 8 (28) (1996) 5235–5245.
- [7] S. Asthana, D. Bahadur, A.K. Nigam, S.K. Malik, Electronic phase separation in $(La_{1/3}Sm_{1/3}A_{1/3})MnO_3$ ($A=Ca, Sr, \text{ and } Ba$) compounds, J. Appl. Phys. 97 (2005) 10H711.
- [8] S. Asthana, D. Bahadur, A.K. Nigam, S.K. Malik, Magneto-transport studies of $(Pr_{1/3}Sm_{1/3}A_{1/3})MnO_3$ ($A=Ca, Sr, \text{ and } Ba$) compounds, J. Phys. Condens. Matter. 16 (29) (2004) 5297–5307.
- [9] S. Asthana, A.K. Nigam, S.K. Malik, D. Bahadur, Lattice effect on the magnetic and magneto-transport properties of $(La_{1/3}Sm_{2/3})_{2/3}Ba_{0.33-x}Sr_xMnO_3$ ($x=0.0, 0.1, 0.2$ and 0.33) compounds, J. Alloys Compd. 450 (1–2) (2008) 136–141.
- [10] S.L. Yuan, G. Li, Y. Jiang, J.Q. Li, X.Y. Zeng, Y.P. Yang, Z. Huang, S.Z. Jin, Exchange-narrowing spin-spin interaction in the paramagnetic regime of perovskite manganites studied through the EPR measurements for $(La, Y)_{2/3}(Ca, Sr, Ba)_{1/3}MnO_3$ with a wide span of T_C , J. Phys.: Condens. Matter 12 (6) (2000) L109–L114.
- [11] S.E. Lofland, P. Kim, P. Dahiroc, S.M. Bhagat, S.D. Tyagi, S.G. Karabashev, D.A. Shulyatev, A.A. Arsenov, Y. Mukovskii, Electron spin resonance measurements in $La_{1-x}Sr_xMnO_3$, Phys. Lett. A 233 (4–6) (1997) 476–480.
- [12] A. Shengelaya, H. Guo-meng Zhao, K.A. Keller, B.I. Muller, E.P.R. Kochelaev, $La_{1-x}Ca_xMnO_3$: relaxation and bottleneck, Phys. Rev. B 61 (9) (2000) 5888–5890.
- [13] C. Rettori, D. Rao, J. Singley, D. Kidwell, S.B. Oseroff, M.T. Causa, J.J. Neumeier, K.J. McClellan, S.-W. Cheong, S. Schultz, Temperature dependence of the ESR linewidth in the paramagnetic phase ($T > T_C$) of $R_{1-x}B_xMnO_{3+\delta}$ ($R=La, Pr, B=Ca, Sr$), Phys. Rev. B 55 (5) (1997) 3083–3086.
- [14] M. Rubinstein, D.J. Gillespie, J.E. Snyder, T.M. Tritt, Effects of Gd, Co and Ni doping in $La_{2/3}Ca_{1/3}MnO_3$: resistivity, thermopower, and paramagnetic resonance, Phys. Rev. B 56 (9) (1997) 5412–5423.
- [15] M.T. Causa, M. Tovar, A. Caneiro, F. Prado, G. Ihañez, C.A. Ramos, A. Butera, A. Alascio, X. Obrados, S. Piñol, F. Rivadulla, C. Vázquez-Vázquez, M.A. Lipez-Quintela, J. Rivas, Y. Tokura, S.B. Oseroff, High-temperature spin dynamics in CMR manganites: ESR and magnetization, Phys. Rev. B 58 (6) (1998) 3233–3239.
- [16] S.V. Gudenko, A. Yu., O. Yakubovskii, Yu. Gorbenco, A.R. Kaul, EPR study of the spin dynamics of the $(La_{1-y}Pr_y)_{0.7}Ca_{0.3}MnO_3$ system, Phys. Solid State 46 (11) (2004) 2094–2102.
- [17] J.P. Joshi, K. Vijaya Sarathy, A.K. Sood, S.V. Bhat, C.N.R. Rao, An electron paramagnetic resonance study of electron-hole asymmetry in charge ordered $Pr_{1-x}Ca_xMnO_3$ ($x=0.64, 0.36$), J. Phys.: Condens. Matter 16 (16) (2004) 2869–2878.
- [18] S.B. Oseroff, M. Torikachvili, J. Singley, S. Ali, S.-W. Cheong, S. Schultz, Evidence for collective spin dynamics above the ordering temperature in $La_{1-x}Ca_xMnO_{3+\delta}$, Phys. Rev. B 53 (10) (1996) 6521–6525.

- [19] M.T. Causa, G. Alejandro, R. Zysler, F. Prado, A. Caneiro, M. Tovar, Jahn–Teller effects on the superexchange interactions in LaMnO_3 , *J. Magn. Magn. Mater.* 196–197 (1999) 506–508.
- [20] A.N. Ulyanov, H.D. Quang, N.E. Pismenova, S.-C. Yu, EPR and resistivity study of $\text{Pr}_{0.7}\text{Ba}_{0.3}\text{MnO}_3$ manganite, *IEEE Trans. Magn.* 41 (10) (2005) 2745–2747.
- [21] R.M. Eremina, J.V. Yatsyk, Ya.M. Mukovskii, H.-A. Krug, A. Von Nidda, Loidl, Determination of the region of existence of ferromagnetic nanostructures in the paraphrase of $\text{La}_{1-x}\text{Ba}_x\text{MnO}_3$ by the EPR method, *JETP Lett.* 85 (1) (2007) 51–54.
- [22] J. Deisenhofer, D. Braak, H.-A. Krug von Nidda, J. Hemberger, R.M. Eremina, V.A. Ivanshin, A.M. Balbashov, G. Jug, A. Loidl, T. Kimura, Y. Tokura, Observation of a griffiths phase in paramagnetic $\text{La}_{1-x}\text{Sr}_x\text{MnO}_3$, *Phys. Rev. Lett.* 95 (25) (2005) 257202.
- [23] X.J. Chen, C.L. Zhang, C.C. Almasan, J.S. Gardner, J.L. Sarrao, Small-polaron hopping conduction in bilayer manganite $\text{La}_{1.2}\text{Sr}_{1.8}\text{Mn}_2\text{O}_7$, *Phys. Rev. B* 67 (9) (2003) 094426.
- [24] Guo-meng Zhao, H Keller, R.L. Greene, K.A. Muller, in: T.A. Kaplan, S.D. Mahanti (Eds.), *Physics of Manganites*, Plenum, New York, 1999, p. 221.
- [25] D.C. Worledge, G. Jeffrey Snyder, M.R. Beasley, T.H. Geballe, R. Hiskes, S. DiCarolis, Anneal-tunable Curie temperature and transport of $\text{La}_{0.67}\text{Ca}_{0.33}\text{MnO}_3$, *J. Appl. Phys.* 80 (9) (1996) 5158–5161.
- [26] R.B. Griffiths, Nonanalytic behavior above the critical point in a random ising ferromagnet, *Phys. Rev. Lett.* 23 (1) (1969) 17–19.
- [27] H. Mori, Transport, collective motion and Brownian motion, *Prog. Theor. Phys.* 33 (3) (1965) 423–455.
- [28] M.T. Causa, M.C.G. Passeggi, Temperature dependence of the EPR spectra of KNiF_3 , *Phys. Lett. A* 98 (5–6) (1983) 291–294.
- [29] O. Chauvet, T. Stoto, L. Zuppiroli, Hopping conduction in a nanometers-size crystalline system: a SiC fiber, *Phys. Rev. B* 46 (13) (1992) 8139–8146.
- [30] C.M. Srivastava, S. Banerjee, T.K. GunduRao, A.K. Nigam, D. Bahadur, Evidence of spin transition and charge order in cobalt substituted $\text{La}_{0.7}\text{Ca}_{0.3}\text{MnO}_3$, *J. Phys. Cond. Matter* 15 (2003) 2375–2388.